Supplementary Material for Anomalous Transport Induced by Non-Hermitian Anomalous Berry Connection in Non-Hermitian Systems

Jiong-Hao Wang[1], Yu-Liang Tao[1], and Yong Xu[1,2*]
[1] *Center for Quantum Information, IIIS, Tsinghua University, Beijing 100084, People's Republic of China and*
[2] *Shanghai Qi Zhi Institute, Shanghai 200030, People's Republic of China*

In the supplementary material, we will show that the velocity of a wave packet is dependent on the Berry curvature defined by right eigenstates in non-Hermitian systems in Section S-1, present the eigenvalues of the Hamiltonian in the main text in Section S-2, discuss the effects of non-Hermitian anomalous Berry connection in a flattened Hamiltonian in Section S-3, analyze the constraints on non-Hermitian anomalous Berry connection imposed by time-reversal symmetry and inversion symmetry or two-fold rotational symmetry in Section S-4, present non-Hermitian anomalous Berry connection in other non-Hermitian models with skin effects in Section S-5, and provide an experimental scheme with coupled resonator optical waveguides in Section S-6.

S-1. RELEVANT BERRY CURVATURE IN NON-HERMITIAN SYSTEMS

In this section, we will show that the velocity of a wave packet is dependent on the Berry curvature defined by right eigenstates.

A. Expectation value of an observable

A quantum non-Hermitian system usually appears due to the system coupled to an environment constituting an open quantum system. Such a system is usually described by the master equation

$$i\partial_t\rho = [H_{eff},\rho]' + \sum_j L_j\rho L_j^\dagger, \tag{S1}$$

where ρ is the density matrix, $[H_{eff},\rho]' = H_{eff}\rho - \rho H_{eff}^\dagger$ with $H_{eff} = H_s - i\frac{1}{2}\sum_j L_j^\dagger L_j$ being an effective non-Hermitian Hamiltonian, H_s is the Hamiltonian of the system, and L_j is the jump operator. If we consider short time dynamics or consider the postselection so that the results corresponding to occurrence of a quantum jump are discarded, the dynamics is governed by

$$i\partial_t\rho = [H_{eff},\rho]'. \tag{S2}$$

If an initial state is a pure state $|\Psi(t=0)\rangle$ $[\rho(t=0) = |\Psi(t=0)\rangle\langle\Psi(t=0)|]$, then the state evolves as $\rho(t) = |\Psi(t)\rangle\langle\Psi(t)|$, where $|\Psi(t)\rangle$ evolves according to

$$i\partial_t|\Psi(t)\rangle = H_{eff}|\Psi(t)\rangle. \tag{S3}$$

The expectation value of an observable O is thus given by

$$\langle O\rangle = \frac{\mathrm{Tr}[O\rho(t)]}{\mathrm{Tr}[\rho(t)]} = \frac{\mathrm{Tr}[O|\Psi(t)\rangle\langle\Psi(t)|]}{\mathrm{Tr}[|\Psi(t)\rangle\langle\Psi(t)|]} = \langle\Psi_1|O|\Psi_1\rangle, \tag{S4}$$

where $|\Psi_1\rangle = |\Psi(t)\rangle/\sqrt{\langle\Psi(t)|\Psi(t)\rangle}$. In the derivation, we have chosen an orthonormal basis including $|\Psi_1\rangle$ for the Hilbert space, $\beta = \{|\Psi_1\rangle, |\Psi_2\rangle, \cdots, |\Psi_N\rangle\}$ (N denotes the dimension of the Hilbert space), so that

$$\mathrm{Tr}[O|\Psi(t)\rangle\langle\Psi(t)|] = \langle\Psi_1|O|\Psi_1\rangle\langle\Psi(t)|\Psi(t)\rangle + \sum_{j=2}^{N}\langle\Psi_j|O|\Psi(t)\rangle\langle\Psi(t)|\Psi_j\rangle = \langle\Psi_1|O|\Psi_1\rangle\langle\Psi(t)|\Psi(t)\rangle. \tag{S5}$$

This tells us that the expectation value is completely determined by the evolving state $|\Psi(t)\rangle$.

In a strongly correlated or disordered system, it has been justified in Ref. [S1] that the effective non-Hermitian Hamiltonian in the single-particle Green's function corresponds to the non-Hermitian Hamiltonian in the context of an open quantum system under postselection, indicating that the expectation value of an observable of a wave packet is still determined by the evolving state $|\Psi(t)\rangle$ under the effective non-Hermitian Hamiltonian.

B. Derivation of the semiclassical equations of motion

We now provide the detailed derivation of the semiclassical dynamics of Bloch electrons (a brief version can be found in the Supplementary Material in Ref. [S2]). Consider a wave packet as an initial state, which can be written in terms of the right Bloch eigenstates of a non-Hermitian Hamiltonian H without an external force as

$$|\Phi(t=0)\rangle = \int_k a(\boldsymbol{k}, t=0)|\phi_n^R(\boldsymbol{k})\rangle, \tag{S6}$$

where $|\phi_n^R(\boldsymbol{k})\rangle = e^{i\boldsymbol{k}\cdot\boldsymbol{r}}|u_n^R(\boldsymbol{k})\rangle$ is the Bloch state with $|u_n^R(\boldsymbol{k})\rangle$ being the right eigenstate of a non-Hermitian Hamiltonian. The wave packet evolves with time as

$$|\Phi(t)\rangle = \int_k a(\boldsymbol{k}, t)|\phi_n^R(\boldsymbol{k})\rangle, \tag{S7}$$

where $a(\boldsymbol{k},t) = |a(\boldsymbol{k},t)|e^{i\gamma(\boldsymbol{k},t)}$ with the amplitude $|a(\boldsymbol{k},t)|$ taking the Gaussian form centered at $\boldsymbol{k}_c = \int_k |a(\boldsymbol{k},t)|^2\boldsymbol{k}/\int_k |a(\boldsymbol{k},t)|^2 = \int_k |a'(\boldsymbol{k},t)|^2\boldsymbol{k}$ where $|a'(\boldsymbol{k},t)|^2 \equiv |a(\boldsymbol{k},t)|^2/\int_{k'}|a(\boldsymbol{k}',t)|^2$ (while $|a(\boldsymbol{k},t)|$ may decrease with time in the presence of a loss term so that $\langle\Phi|\Phi\rangle = \int_k |a(\boldsymbol{k},t)|^2 < 1$, we can evaluate the expectation value of an observable by mutiplying a factor $1/\langle\Phi|\Phi\rangle$).

Let us first derive the expression of $\gamma(\boldsymbol{k},t)$ which contains both dynamical and geometric phases. In the presence of an external force, the Schrödinger equation reads

$$i\partial_t|\psi(t)\rangle = (H - \boldsymbol{F}\cdot\hat{\boldsymbol{r}})|\psi(t)\rangle. \tag{S8}$$

Consider a Bloch eigenstate at $\boldsymbol{k}_0$ as an initial state at time t_0 and suppose that the external force is sufficiently weak so that the evolving state is still a Bloch eigenstate multiplied by a factor, that is,

$$|\psi(t)\rangle = \alpha(t)|\phi^R_{n\boldsymbol{k}(t)}\rangle = \alpha(t)e^{i\boldsymbol{k}(t)\cdot\boldsymbol{r}}|u^R_{n\boldsymbol{k}(t)}\rangle \tag{S9}$$

$$\boldsymbol{k}(t) = \boldsymbol{k}_0 + \boldsymbol{F}t. \tag{S10}$$

We now substitute $|\psi(t)\rangle$ into the Schrödinger equation, yielding

$$\begin{aligned}
i\partial_t|\psi(t)\rangle =& ie^{i\boldsymbol{k}(t)\cdot\boldsymbol{r}}|u_n^R(\boldsymbol{k}(t))\rangle\partial_t\alpha(t) - \alpha(t)e^{i\boldsymbol{k}(t)\cdot\boldsymbol{r}}|u_n^R(\boldsymbol{k}(t))\rangle\boldsymbol{F}\cdot\boldsymbol{r} + i\alpha(t)e^{i\boldsymbol{k}(t)\cdot\boldsymbol{r}}\partial_t|u_n^R(\boldsymbol{k}(t))\rangle & \text{(S11)}\\
=&(H - \boldsymbol{F}\cdot\hat{\boldsymbol{r}})|\psi(t)\rangle & \text{(S12)}\\
=&\alpha(t)\hat{H}e^{i\boldsymbol{k}(t)\cdot\boldsymbol{r}}|u_n^R(\boldsymbol{k}(t))\rangle - \alpha(t)e^{i\boldsymbol{k}(t)\cdot\boldsymbol{r}}|u_n^R(\boldsymbol{k}(t))\rangle\boldsymbol{F}\cdot\boldsymbol{r} & \text{(S13)}\\
=&\alpha(t)\varepsilon_n(\boldsymbol{k}(t))e^{i\boldsymbol{k}(t)\cdot\boldsymbol{r}}|u_n^R(\boldsymbol{k}(t))\rangle - \alpha(t)e^{i\boldsymbol{k}(t)\cdot\boldsymbol{r}}|u_n^R(\boldsymbol{k}(t))\rangle\boldsymbol{F}\cdot\boldsymbol{r}. & \text{(S14)}
\end{aligned}$$

We thus obtain

$$i|u_n^R(\boldsymbol{k}(t))\rangle\partial_t\alpha(t) = \alpha(t)\varepsilon_n(\boldsymbol{k}(t))|u_n^R(\boldsymbol{k}(t))\rangle - i\alpha(t)\partial_t|u_n^R(\boldsymbol{k}(t))\rangle. \tag{S15}$$

To derive the equation satisfied by $\alpha(t)$, we consider any state written as a linear combination of the left eigenstates $|u_j^L(\boldsymbol{k}(t))\rangle$ [note that $\{|u_j^L(\boldsymbol{k}(t))\rangle\}$ constitute an ordered basis, although it may not be orthogonal], that is,

$$|u'_{\boldsymbol{k}(t)}\rangle = c_n^*|u_n^L(\boldsymbol{k}(t))\rangle + \sum_{j\neq n} c_j^*|u_j^L(\boldsymbol{k}(t))\rangle. \tag{S16}$$

We then multiply Eq. (S15) by $\langle u'_{\boldsymbol{k}(t)}|$, resulting in

$$ic_n\partial_t\alpha(t) = c_n\alpha(t)[\varepsilon_n(\boldsymbol{k}(t)) - i\langle u_n^L(\boldsymbol{k}(t))|\partial_t|u_n^R(\boldsymbol{k}(t))\rangle] - i\alpha(t)\sum_{j\neq n} c_j\langle u_j^L(\boldsymbol{k}(t))|\partial_t|u_n^R(\boldsymbol{k}(t))\rangle, \tag{S17}$$

where we have used the biorthogonal relation $\langle u_m^L(\boldsymbol{k})|u_n^R(\boldsymbol{k})\rangle = \delta_{mn}$. The final term vanishes because multiplying Eq. (S15) by $\sum_{j\neq n} c_j\langle u_j^L(\boldsymbol{k}(t))|$ yields

$$\alpha(t)\sum_{j\neq n} c_j\langle u_j^L(\boldsymbol{k}(t))|\partial_t|u_n^R(\boldsymbol{k}(t))\rangle = 0. \tag{S18}$$

Thus, we obtain

$$i\partial_t\alpha(t) = \alpha(t)\varepsilon_n(\boldsymbol{k}(t)) - i\alpha(t)\langle u_n^L(\boldsymbol{k}(t))|\partial_t|u_n^R(\boldsymbol{k}(t))\rangle = \alpha(t)\left[\varepsilon_n(\boldsymbol{k}(t)) - \tilde{\boldsymbol{A}}_{n\boldsymbol{k}(t)}\cdot\boldsymbol{F}\right], \tag{S19}$$

yielding

$$\alpha(t) = e^{-i\int_{t_0}^{t} dt'\left[\varepsilon_n(\boldsymbol{k}(t'))-\tilde{\boldsymbol{A}}_n(\boldsymbol{k}(t'))\cdot\boldsymbol{F}\right]}, \tag{S20}$$

where $\tilde{\boldsymbol{A}}_n(\boldsymbol{k}(t)) = i\langle u_n^L(\boldsymbol{k})|\partial_{\boldsymbol{k}}u_n^R(\boldsymbol{k})\rangle|_{\boldsymbol{k}=\boldsymbol{k}(t)}$ is the left-right Berry connection contributing to the geometric phase.

We note that in the derivation, while one can also use the right eigenvectors to generate $|u'_{\boldsymbol{k}(t)}\rangle$, that is,

$$|u'_{\boldsymbol{k}(t)}\rangle = b_n^*|u_n^R(\boldsymbol{k}(t))\rangle + \sum_{j\neq n} b_j^*|u_j^R(\boldsymbol{k}(t))\rangle, \tag{S21}$$

multiplying Eq. (S15) by this expansion cannot give us an equation as concise as Eq. (S19) due to the absence of an orthogonal relation for right eigenvectors in non-Hermitian systems [$\langle u_m^R(\boldsymbol{k})|u_n^R(\boldsymbol{k})\rangle$ usually does not vanish if $m \neq n$]. Note here we consider a system without exceptional points; otherwise, neither right eigenvectors nor left eigenvectors can constitute a basis for the Hilbert space.

We are now in a position to derive the center of mass of the wave packet in real space as time evolves based on Eq. (S7); the location of the wave packet is given by

$$\begin{aligned}
&\boldsymbol{r}_c(t)\\
=&\langle\Phi(t)|\hat{\boldsymbol{r}}|\Phi(t)\rangle/\langle\Phi(t)|\Phi(t)\rangle && \text{(S22)}\\
=&\int d\boldsymbol{r}\int_k\int_{k'}|a(\boldsymbol{k}',t)||a(\boldsymbol{k},t)|e^{i\gamma(\boldsymbol{k},t)}e^{-i\gamma(\boldsymbol{k}',t)}e^{-i\boldsymbol{k}'\cdot\boldsymbol{r}}[u_{n\boldsymbol{k}'}^R(\boldsymbol{r})]^\dagger\boldsymbol{r}e^{i\boldsymbol{k}\cdot\boldsymbol{r}}u_{n\boldsymbol{k}}^R(\boldsymbol{r})/\langle\Phi|\Phi\rangle && \text{(S23)}\\
=&\int d\boldsymbol{r}\int_k\int_{k'}|a(\boldsymbol{k}',t)||a(\boldsymbol{k},t)|e^{i\gamma(\boldsymbol{k},t)}e^{-i\gamma(\boldsymbol{k}',t)}e^{i(\boldsymbol{k}-\boldsymbol{k}')\cdot\boldsymbol{r}}\boldsymbol{r}[u_{n\boldsymbol{k}'}^R(\boldsymbol{r})]^\dagger u_{n\boldsymbol{k}}^R(\boldsymbol{r})/\langle\Phi|\Phi\rangle && \text{(S24)}\\
=&\int_k\int_{k'}\int d\boldsymbol{r}|a(\boldsymbol{k}',t)||a(\boldsymbol{k},t)|e^{i\gamma(\boldsymbol{k},t)}e^{-i\gamma(\boldsymbol{k}',t)}[u_{n\boldsymbol{k}'}^R(\boldsymbol{r})]^\dagger u_{n\boldsymbol{k}}^R(\boldsymbol{r})(-i\partial_{\boldsymbol{k}})e^{i(\boldsymbol{k}-\boldsymbol{k}')\cdot\boldsymbol{r}}/\langle\Phi|\Phi\rangle && \text{(S25)}\\
=&\int_k\int_{k'}\int d\boldsymbol{r}e^{i(\boldsymbol{k}-\boldsymbol{k}')\cdot\boldsymbol{r}}|a(\boldsymbol{k}',t)|e^{-i\gamma(\boldsymbol{k}',t)}[u_{n\boldsymbol{k}'}^R(\boldsymbol{r})]^\dagger i\partial_{\boldsymbol{k}}|a(\boldsymbol{k},t)|e^{i\gamma(\boldsymbol{k},t)}u_{n\boldsymbol{k}}^R(\boldsymbol{r})/\langle\Phi|\Phi\rangle && \text{(S26)}\\
=&\int_k\int d\boldsymbol{r}|a(\boldsymbol{k},t)|e^{-i\gamma(\boldsymbol{k},t)}[u_{n\boldsymbol{k}}^R(\boldsymbol{r})]^\dagger i\partial_{\boldsymbol{k}}|a(\boldsymbol{k},t)|e^{i\gamma(\boldsymbol{k},t)}u_{n\boldsymbol{k}}^R(\boldsymbol{r})/\langle\Phi|\Phi\rangle && \text{(S27)}\\
=&\int_k\int d\boldsymbol{r}|a(\boldsymbol{k},t)|e^{-i\gamma(\boldsymbol{k},t)}[u_{n\boldsymbol{k}}^R(\boldsymbol{r})]^\dagger\left[e^{i\gamma(\boldsymbol{k},t)}u_{n\boldsymbol{k}}^R(\boldsymbol{r})i\partial_{\boldsymbol{k}}|a(\boldsymbol{k},t)| - (\partial_{\boldsymbol{k}}\gamma(\boldsymbol{k},t))|a(\boldsymbol{k},t)|e^{i\gamma(\boldsymbol{k},t)}u_{n\boldsymbol{k}}^R(\boldsymbol{r})+\right. && \text{(S28)}\\
&\left.|a(\boldsymbol{k},t)|e^{i\gamma(\boldsymbol{k},t)}(i\partial_{\boldsymbol{k}})u_{n\boldsymbol{k}}^R(\boldsymbol{r})\right]/\langle\Phi|\Phi\rangle && \text{(S29)}\\
=&\int_k|a(\boldsymbol{k},t)|i\partial_{\boldsymbol{k}}|a(\boldsymbol{k},t)|/\langle\Phi|\Phi\rangle - \int_k|a(\boldsymbol{k},t)|^2(\partial_{\boldsymbol{k}}\gamma(\boldsymbol{k},t))/\langle\Phi|\Phi\rangle + \int_k|a(\boldsymbol{k},t)|^2\int d\boldsymbol{r}[u_{n\boldsymbol{k}}^R(\boldsymbol{r})]^\dagger i\partial_{\boldsymbol{k}}u_{n\boldsymbol{k}}^R(\boldsymbol{r})/\langle\Phi|\Phi\rangle && \text{(S30)}\\
=&-\int_k|a'(\boldsymbol{k},t)|^2\partial_{\boldsymbol{k}}\gamma(\boldsymbol{k},t) + \int_k|a'(\boldsymbol{k},t)|^2\int d\boldsymbol{r}[u_{n\boldsymbol{k}}^R(\boldsymbol{r})]^\dagger i\partial_{\boldsymbol{k}}u_{n\boldsymbol{k}}^R(\boldsymbol{r}) && \text{(S31)}\\
=&-\int_k|a'(\boldsymbol{k},t)|^2\partial_{\boldsymbol{k}}\gamma(\boldsymbol{k},t) + \int_k|a'(\boldsymbol{k},t)|^2\langle u_{n\boldsymbol{k}}^R|i\partial_{\boldsymbol{k}}|u_{n\boldsymbol{k}}^R\rangle && \text{(S32)}\\
\approx&-\frac{\partial\gamma(\boldsymbol{k}_c,t)}{\partial\boldsymbol{k}_c} + i\langle u_{n\boldsymbol{k}_c}^R|\partial_{\boldsymbol{k}_c}|u_{n\boldsymbol{k}_c}^R\rangle && \text{(S33)}\\
=&-\frac{\partial\gamma(\boldsymbol{k}_c,t)}{\partial\boldsymbol{k}_c} + \boldsymbol{A}_n(\boldsymbol{k}_c), && \text{(S34)}
\end{aligned}$$

where $\boldsymbol{A}_n(\boldsymbol{k}_c) = i\langle u_{n\boldsymbol{k}_c}^R|\partial_{\boldsymbol{k}_c}|u_{n\boldsymbol{k}_c}^R\rangle$ is the right-right Berry connection with $|u_{n\boldsymbol{k}_c}^R\rangle \equiv |u_n^R(\boldsymbol{k}_c)\rangle$. With the aid of Eq. (S20), we have

$$\gamma(\boldsymbol{k}_c,t) = -\int_{t_0}^{t} dt'\mathrm{Re}\left[\varepsilon_n(\boldsymbol{k}(t')) - \tilde{\boldsymbol{A}}_n(\boldsymbol{k}(t'))\cdot\boldsymbol{F}\right].$$

We thus can derive the velocity of the wave packet as

$$\begin{aligned}
\boldsymbol{v}_c(t_0) &= \frac{\boldsymbol{r}_c(t_0+\delta t)-\boldsymbol{r}_c(t_0)}{\delta t} \\
&= \partial_{\boldsymbol{k}_c}\frac{\delta t\left[\mathrm{Re}[\varepsilon_n(\boldsymbol{k}_c)]-\mathrm{Re}[\tilde{\boldsymbol{A}}_n(\boldsymbol{k}_c)]\cdot\boldsymbol{F}\right]}{\delta t}+\frac{d\boldsymbol{A}_n(\boldsymbol{k}_c)}{dt}|_{t=t_0} \\
&= \partial_{\boldsymbol{k}_c}\mathrm{Re}[\varepsilon_n(\boldsymbol{k}_c)]-\partial_{\boldsymbol{k}_c}\mathrm{Re}[\tilde{A}_{n,\nu}(\boldsymbol{k}_c)]\cdot F_\nu+\frac{d\boldsymbol{A}_n(\boldsymbol{k}_c)}{dt}|_{t=t_0} \\
&= \partial_{\boldsymbol{k}_c}\mathrm{Re}[\varepsilon_n(\boldsymbol{k}_c)]-(\partial_{\boldsymbol{k}_c}\mathrm{Re}[\tilde{A}_{n,\nu}(\boldsymbol{k}_c)])\cdot\dot{k}_{c,\nu}+\frac{d\boldsymbol{A}_n(\boldsymbol{k}_c)}{dt}|_{t=t_0}, \\
&= \partial_{\boldsymbol{k}_c}\mathrm{Re}[\varepsilon_n(\boldsymbol{k}_c)]-\partial_{\boldsymbol{k}_c}A_{n,\nu}(\boldsymbol{k}_c)\cdot\dot{k}_{c,\nu}+\frac{d\boldsymbol{A}_n(\boldsymbol{k}_c)}{dt}|_{t=t_0}+\partial_{\boldsymbol{k}_c}\left[A_{n,\nu}(\boldsymbol{k}_c)-\mathrm{Re}\tilde{A}_{n,\nu}(\boldsymbol{k}_c)\right]\cdot\dot{k}_{c,\nu} \\
&= \partial_{\boldsymbol{k}_c}\mathrm{Re}[\varepsilon_n(\boldsymbol{k}_c)]-\dot{\boldsymbol{k}}_c\times\boldsymbol{\Omega}+\partial_{\boldsymbol{k}_c}\mathrm{Re}\left[A_{n,\nu}(\boldsymbol{k}_c)-\tilde{A}_{n,\nu}(\boldsymbol{k}_c)\right]\cdot\dot{k}_{c,\nu} \\
&= \partial_{\boldsymbol{k}_c}\mathrm{Re}[\varepsilon_n(\boldsymbol{k}_c)]-\dot{\boldsymbol{k}}_c\times\boldsymbol{\Omega}+\partial_{\boldsymbol{k}_c}\bar{A}_{n,\nu}(\boldsymbol{k}_c)\cdot\dot{k}_{c,\nu} \\
&= \partial_{\boldsymbol{k}_c}[\mathrm{Re}[\varepsilon_n(\boldsymbol{k}_c)]+\bar{A}_{n,\nu}(\boldsymbol{k}_c)\cdot\dot{k}_{c,\nu}]-\dot{\boldsymbol{k}}_c\times\boldsymbol{\Omega},
\end{aligned}$$

where $\bar{A}_{n,\nu}(\boldsymbol{k}_c)\equiv\mathrm{Re}\left[A_{n,\nu}(\boldsymbol{k}_c)-\tilde{A}_{n,\nu}(\boldsymbol{k}_c)\right]$ and $\boldsymbol{\Omega}=i\langle\nabla_{\boldsymbol{k}}u_n^R(\boldsymbol{k})|\times|\nabla_{\boldsymbol{k}}u_n^R(\boldsymbol{k})\rangle$. In the derivation, we have used the fact that $\boldsymbol{F}=\dot{\boldsymbol{k}}$. We can clearly see that the velocity of a wave packet is dependent on the right-right Berry curvature, which is independent of the left eigenstates.

S-2. EIGENENERGIES OF THE HAMILTONIAN

The Hamiltonian (5) in the main text is pseudo-Hermitian, i.e., $U^{-1}HU=H^\dagger$ with $U=\mathrm{diag}(\sqrt{q},1/\sqrt{q})$, and its eigenenergies are real, $\varepsilon_\pm=mc_0+\xi_\pm$ with $\xi_\pm=\pm\sqrt{ab(d_x^2+d_y^2)+m^2c_1^2}$ and $c_0=(1-q^2)/(2q)$ and $c_1=(1+q^2)/(2q)$.

S-3. EFFECTS OF NON-HERMITIAN ANOMALOUS BERRY CONNECTION IN A FLATTENED HAMILTONIAN

To illustrate the non-Hermitian anomalous Berry connection effects, we can take a limit and consider a flattened Hamiltonian

$$H_{\mathrm{F}}=|u_+^R\rangle\langle u_+^L|-|u_-^R\rangle\langle u_-^L|, \tag{S35}$$

where $|u_\pm^R\rangle$ and $\langle u_\pm^L|$ are the normalized right and left eigenstates of the Hamiltonian (5), respectively, corresponding to eigenenergy $\varepsilon_\pm$. For the flattened Hamiltonian, its eigenenergies are $\varepsilon_{\mathrm{F},\pm}=\pm1$, which is independent of quasimomentum k and thus the group velocity contributed by the energy dispersion vanishes. However, the non-Hermitian anomalous velocity remains the same as in the Hamiltonian (5), since it only depends on the wave functions. In this case, we can clearly see that even though the traditional semiclassical equations of motion predict the absence of motion for an electron in the presence of an external electric field, our theory indicates that the electron can still move due to the emergence of a velocity arising from the non-Hermiticity and local geometric effects. More interestingly, given that $\boldsymbol{v}_{\mathrm{NA}}$ is proportional to the electric field, one can control the direction of the velocity of an electron by suddenly reversing the direction of the electric field.

S-4. SYMMETRY CONSTRAINTS ON NON-HERMITIAN ANOMALOUS BERRY CONNECTION

In this section, we explore the constraints on non-Hermitian anomalous Berry connection imposed by time-reversal symmetry and inversion or two-fold rotational symmetry.

A. Time-reversal symmetry

For a non-Hermitian system, time-reversal and particle-hole symmetries develop into four categories [S3, S4]:

$$T_\pm H^*(-\boldsymbol{k})T_\pm^\dagger = \pm H(\boldsymbol{k}) \tag{S36}$$

$$\Xi_\pm H^T(-\boldsymbol{k})\Xi_\pm^\dagger = \pm H(\boldsymbol{k}), \tag{S37}$$

where $T_\pm$ and $\Xi_\pm$ are unitary operators. The Hamiltonian (5) in the main text respects the time-reversal symmetry with T_+ being an identity matrix. We thus only consider the constraint imposed by T_+ with $T_+T_+^* = 1$.

Let $|u_n^R(\boldsymbol{k})\rangle$ and $\langle u_n^L(\boldsymbol{k})|$ be the normalized right and left eigenstate of a non-Hermitian Hamiltonian $H(\boldsymbol{k})$ in the nth band corresponding to an eigenvalue $\varepsilon_n(\boldsymbol{k})$, respectively, that is, $H(\boldsymbol{k})|u_n^R(\boldsymbol{k})\rangle = \varepsilon_k|u_n^R(\boldsymbol{k})\rangle$ and $\langle u_n^L(\boldsymbol{k})|H(\boldsymbol{k}) = \varepsilon_k\langle u_n^L(k)|$. Based on the symmetry constraint, one can easily obtain

$$H(-\boldsymbol{k})T_+|u_n^R(\boldsymbol{k})\rangle^* = T_+T_+^\dagger H(-\boldsymbol{k})T_+|u_n^R(\boldsymbol{k})\rangle^* = T_+H^*(\boldsymbol{k})|u_n^R(\boldsymbol{k})\rangle^* = \varepsilon_n^*(\boldsymbol{k})T_+|u_n^R(\boldsymbol{k})\rangle^*, \tag{S38}$$

and

$$(\langle u_n^L(\boldsymbol{k})|)^*T_+^\dagger H(-\boldsymbol{k}) = (\langle u_n^L(\boldsymbol{k})|)^*H^*(\boldsymbol{k})T_+^\dagger = \varepsilon_n^*(\boldsymbol{k})(\langle u_n^L(\boldsymbol{k})|)^*T_+^\dagger, \tag{S39}$$

indicating that $T_+|u_n^R(\boldsymbol{k})\rangle^*$ and $(\langle u_n^L(\boldsymbol{k})|)^*T_+^\dagger$ are the right and left eigenstates of $H(-\boldsymbol{k})$ with eigenvalue $\varepsilon_n^*(\boldsymbol{k})$, respectively. Since non-Hermitian anomalous Berry connection is gauge independent, we choose a gauge so that $|u_n^R(-\boldsymbol{k})\rangle = T_+|u_n^R(\boldsymbol{k})\rangle^*$ and $\langle u_n^L(-\boldsymbol{k})| = (\langle u_n^L(\boldsymbol{k})|)^*T_+^\dagger$, which fulfill the normalization condition $\langle u_n^R(-\boldsymbol{k})|u_n^R(-\boldsymbol{k})\rangle = 1$ and $\langle u_n^L(-\boldsymbol{k})|u_n^R(-\boldsymbol{k})\rangle = 1$. We now derive the constraints as

$$A_{n,\mu}(-\boldsymbol{k}) = -i\langle u_n^R(-\boldsymbol{k})|\partial_\mu u_n^R(-\boldsymbol{k})\rangle \tag{S40}$$

$$= -i(T_+|u_n^R(\boldsymbol{k})\rangle^*)^\dagger T_+|\partial_\mu u_n^R(\boldsymbol{k})\rangle^* \tag{S41}$$

$$= -i(\langle u_n^R(\boldsymbol{k})|)^*|\partial_\mu u_n^R(\boldsymbol{k})\rangle^* \tag{S42}$$

$$= (A_{n,\mu}(\boldsymbol{k}))^*, \tag{S43}$$

and

$$\tilde{A}_{n,\mu}(-\boldsymbol{k}) = -i\langle u_n^L(-\boldsymbol{k})|\partial_\mu u_n^R(-\boldsymbol{k})\rangle = -i\langle u_n^L(\boldsymbol{k})|^*T_+^\dagger T_+\partial_\mu|u_n^R(\boldsymbol{k})\rangle^* = (\tilde{A}_{n,\mu}(\boldsymbol{k}))^*, \tag{S44}$$

which yield

$$\bar{\boldsymbol{A}}_n(-\boldsymbol{k}) = \bar{\boldsymbol{A}}_n(\boldsymbol{k}). \tag{S45}$$

We thus conclude that the time-reversal symmetry T_+ with $T_+T_+^* = 1$ ensures that non-Hermitian Berry connection $\bar{\boldsymbol{A}}$ is an even function with respect to $\boldsymbol{k}$.

B. Inversion symmetry or two-fold rotational symmetry

We now consider inversion symmetry or two-fold rotational symmetry which forces the Hamiltonian to respect

$$UH(-\boldsymbol{k})U^\dagger = H(\boldsymbol{k}), \tag{S46}$$

where U is a unitary operator. One can easily find that $U^\dagger|u_n^R(\boldsymbol{k})\rangle$ and $\langle u_n^L(\boldsymbol{k})|U$ are the right and left eigenstates of $H(-\boldsymbol{k})$ corresponding to eigenenergy $\varepsilon_n(\boldsymbol{k})$, respectively. By choosing a gauge so that $|u_n^R(-\boldsymbol{k})\rangle = U^\dagger|u_n^R(\boldsymbol{k})\rangle$ and $\langle u_n^L(-\boldsymbol{k})| = \langle u_n^L(\boldsymbol{k})|U$, one can derive that

$$\boldsymbol{A}_n(-\boldsymbol{k}) = -\boldsymbol{A}_n(\boldsymbol{k}) \tag{S47}$$

$$\tilde{\boldsymbol{A}}_n(-\boldsymbol{k}) = -\tilde{\boldsymbol{A}}_n(\boldsymbol{k}), \tag{S48}$$

leading to

$$\bar{\boldsymbol{A}}_n(-\boldsymbol{k}) = -\bar{\boldsymbol{A}}_n(\boldsymbol{k}). \tag{S49}$$

This tells us that inversion symmetry maintains that non-Hermitian anomalous Berry connection is antisymmetric with respect to $\boldsymbol{k}$. If a system has both time-reversal symmetry T_+ and inversion or two-fold rational symmetry, then non-Hermitian anomalous Berry connection is forced to vanish.

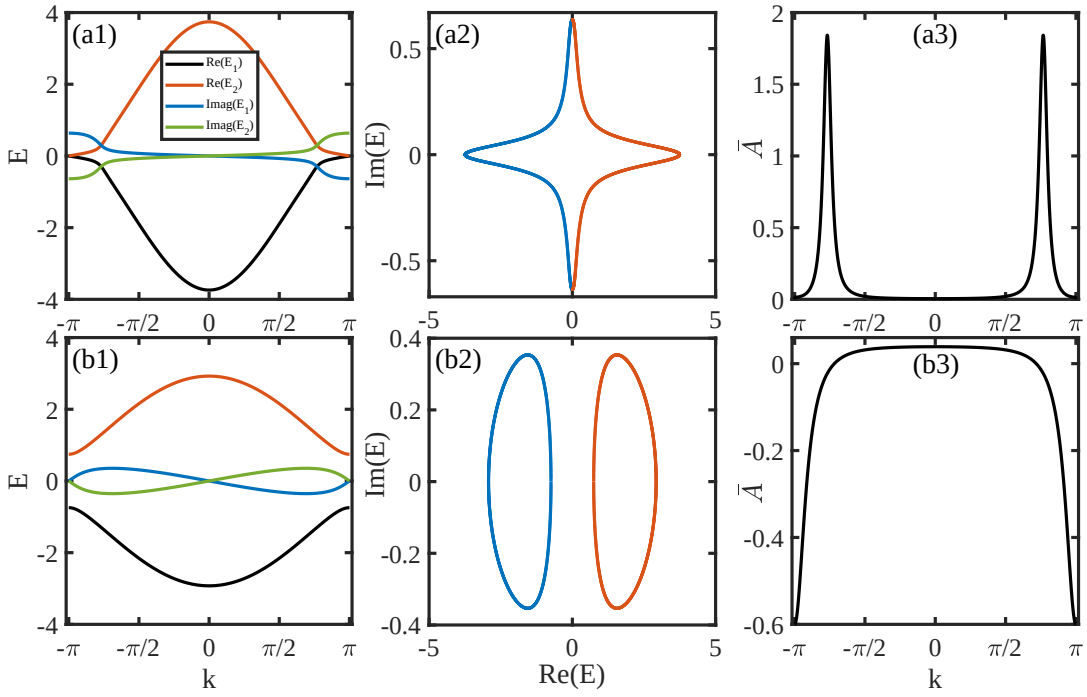

FIG. S1: (Color online) (a1)(b1) Real and imaginary parts of energy spectra with respect to quasimomenta k for the Hamiltonian (S54) with the corresponding energy spectra in the complex plane plotted in (a2) and (b2), respectively. (a3)(b3) NHABC as a function of quasimomenta k. In (a1-a3), $t_1 = 2$, $t_2 = 1$, $t_3 = 0.8$ and $\gamma = 4/3$, and in (b1-b3), $t_1 = 2$, $t_2 = 1$, $t_3 = 0$ and $\gamma = 4/3$.

C. $C_2\mathcal{T}$ or $\mathcal{PT}$ symmetry

For the $C_2\mathcal{T}$ (product of two-fold rotational symmetry and time-reversal symmetry) or $\mathcal{PT}$ (product of inversion symmetry and time-reversal symmetry) symmetry, the Hamiltonian should satisfy

$$UT_+ H(\boldsymbol{k})^* (UT_+)^\dagger = H(\boldsymbol{k}), \tag{S50}$$

where UT_+ is a unitary operator. We consider the case that $(UT_+)(UT_+)^* = 1$. Similarly, one can find that $UT_+|u_n^R(\boldsymbol{k})\rangle^*$ and $(\langle u_n^L(\boldsymbol{k})|)^*(UT_+)^\dagger$ are the right and left eigenstates of $H(\boldsymbol{k})$ corresponding to eigenenergy $\varepsilon_n^*(\boldsymbol{k})$, respectively. If a system is in a $C_2\mathcal{T}$ or $\mathcal{PT}$ symmetric state, that is, $UT_+|u_n^R(\boldsymbol{k})\rangle^* = \alpha^*|u_n^R(\boldsymbol{k})\rangle$ and $\langle u_n^L(\boldsymbol{k})|^*(UT_+)^\dagger = \alpha\langle u_n^L(\boldsymbol{k})|$ with $|\alpha| = 1$, then one can easily derive

$$A_{n,\mu}(\boldsymbol{k}) = i\alpha^*\partial_\mu\alpha - (A_{n,\mu}(\boldsymbol{k}))^* \tag{S51}$$

$$\tilde{A}_{n,\mu}(\boldsymbol{k}) = i\alpha^*\partial_\mu\alpha - (\tilde{A}_{n,\mu}(\boldsymbol{k}))^*, \tag{S52}$$

so that

$$\bar{\boldsymbol{A}}_n(\boldsymbol{k}) = -\bar{\boldsymbol{A}}_n(\boldsymbol{k}), \tag{S53}$$

forcing non-Hermitian anomalous Berry connection to vanish.

S-5. NON-HERMITIAN ANOMALOUS BERRY CONNECTIONS IN OTHER MODELS

In the main text, we consider a model with pseudo-Hermiticity symmetry that exhibits large NHABC. In fact, the NHABC is generically nonzero in a non-Hermitian system. Here, we show that NHABC can be large in other well-known models with skin effects [S5, S6],

$$H(k) = d_x\sigma_x + (d_y + i\gamma/2)\sigma_y, \tag{S54}$$

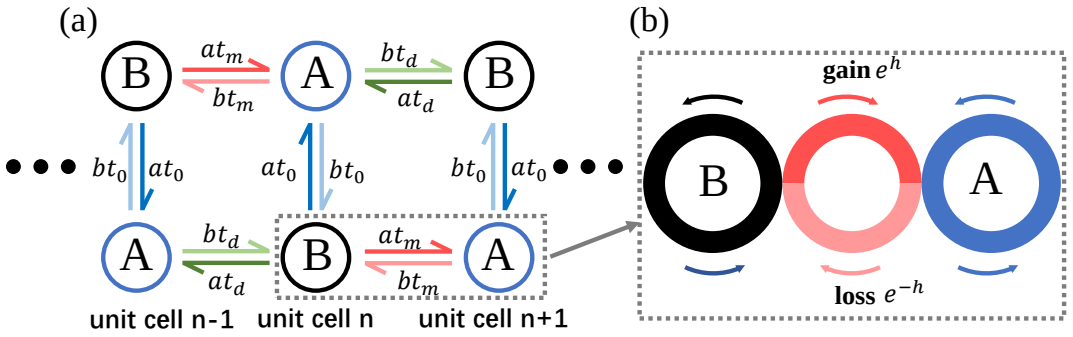

FIG. S2: (Color online) (a) Lattice configurations to realize the Hamiltonian (5) in the main text. Circles labeled by A and B represent site resonators. The effective hopping between the site resonators is generated by a link waveguide (red circle) connecting two neighboring site resonators (black and blue circles) as shown in (b). When gain and loss are involved in link waveguides, the required asymmetric hopping can be realized.

where $d_x = t_1 + (t_2 + t_3)\cos(k)$ and $d_y = (t_2 - t_3)\sin(k)$ with t_1, t_2, t_3 and γ being real parameters describing the corresponding hopping strength.

To show that NHABC has significant effects, we consider two typical cases with $t_1 = 2$, $t_2 = 1$, $t_3 = 0.8$ and $\gamma = 4/3$, and $t_1 = 2$, $t_2 = 1$, $t_3 = 0$ and $\gamma = 4/3$. The system exhibits non-Hermitian skin effects under open boundary conditions since the energy spectra in the complex plane in momentum space [see Fig. S1(a2) and (b2)] have nonzero winding. Figure S1(a3) and (b3) further illustrate that the NHABC is also in the order of one in these systems, similar to the case shown in Fig. 1(a) in the main text for a pseudo-Hermitian Hamiltonian.

S-6. AN EXPERIMENTAL SCHEME WITH COUPLED RESONATOR OPTICAL WAVEGUIDES

To experimentally realize the Hamiltonian (5) with $d_z = d_0 = 0$, $d_x = t_0 + t_1 \cos k$ and $d_y = t_2 \sin k$, we first write down the Hamiltonian in real space

$$H = \sum_n \Big[(\,|A_n\rangle \;\; |B_n\rangle\,) \begin{pmatrix} 0 & at_0 \\ bt_0 & 0 \end{pmatrix} \begin{pmatrix} \langle A_n| \\ \langle B_n| \end{pmatrix} + (\,|A_n\rangle \;\; |B_n\rangle\,) \begin{pmatrix} 0 & at_d \\ bt_m & 0 \end{pmatrix} \begin{pmatrix} \langle A_{n+1}| \\ \langle B_{n+1}| \end{pmatrix} + (\,|A_{n+1}\rangle \;\; |B_{n+1}\rangle\,) \begin{pmatrix} 0 & at_m \\ bt_d & 0 \end{pmatrix} \begin{pmatrix} \langle A_n| \\ \langle B_n| \end{pmatrix} \Big], \tag{S55}$$

where $|A_n\rangle$ and $|B_n\rangle$ denote the state at site A and B in the nth unit cell, respectively, $t_m = (t_1 + t_2)/2$ and $t_d = (t_1 - t_2)/2$. To realize the Hamiltonian in coupled-resonator optical waveguides (CROWs), we consider a configuration for site resonators and link waveguides as illustrated in Fig. S2(a), where A and B sites are interchanged in positions between two neighboring unit cells to realize the next-nearest neighbor hopping between two neighboring unit cells. The hopping between two neighboring sites are implemented by coupling two site resonators (denoted by black and blue circles) with a link waveguide (denoted by a red circle), as shown in Fig. S2(b). In the non-Hermitian case, the asymmetric hopping between two sites can be realized by applying either gain e^h or loss e^{-h} over half circle for a light travelling in a link waveguide [S7]. For instance, consider a light propagating counterclockwise in a site resonator and a gain in the upper semicircle and a loss in the lower semicircle in a link waveguide (see Fig. S2(b)). Such a gain or loss changes the transfer matrix of a link waveguide from left to right by a factor of e^h, resulting in an effective hopping from κ to κe^h, where κ refers to the hopping when $h = 0$. Similarly, the effective hopping from right to left is modified by a factor of e^{-h}.

The dynamics of a wave function is governed by

$$i\partial_t|\Psi\rangle = H|\Psi\rangle + \sum_n (\omega_n - \bar{\omega}) \begin{pmatrix} a_n|A_n\rangle \\ b_n|B_n\rangle \end{pmatrix} - i\gamma|\Psi\rangle, \tag{S56}$$

where

$$|\Psi\rangle = \sum_n \begin{pmatrix} a_n|A_n\rangle \\ b_n|B_n\rangle \end{pmatrix} \tag{S57}$$

with a_n (b_n) denoting the electric field of the light in the A (B) site resonator in the nth unit cell, γ is the global decay rate of the field, and $\omega_n = \bar{\omega} + \delta\omega_n$ represents the resonant frequency of each site resonator. To simulate an external gradient potential, each site resonator is engineered to have a resonant frequency of $\bar{\omega} + \delta\omega_n$ with $\delta\omega_n = \mathcal{E}n$. One can also realize an external ac electric field by controlling local refractive index [S8, S9].

* Electronic address: yongxuphy@tsinghua.edu.cn

[S1] Y. Michishita and R. Peters, Phys. Rev. Lett. **124,** 196401 (2020).
[S2] Y. Xu, S.-T. Wang, and L.-M. Duan, Phys. Rev. Lett. **118,** 045701 (2017).
[S3] K. Kawabata, K. Shiozaki, M. Ueda, and M. Sato, Phys. Rev. X **9,** 041015 (2019).
[S4] H. Zhou and J. Y. Lee, Phys. Rev. B **99,** 235112 (2019).
[S5] T. E. Lee, Phys. Rev. Lett. **116,** 133903 (2016).
[S6] S. Yao and Z. Wang, Phys. Rev. Lett. **121,** 086803 (2018).
[S7] S. Longhi, D. Gatti, and G. D. Valle, Sci. Rep. **5,** 13376 (2015).
[S8] M. F. Yanik and S. Fan, Phys. Rev. Lett. **92,** 083901 (2004).
[S9] S. Longhi, Phys. Rev. E **75,** 026606 (2007).